Serotonin 2C receptors in pro-opiomelanocortin neurons regulate energy and glucose homeostasis

Eric D. Berglund,[1] Chen Liu,[1] Jong-Woo Sohn,[1] Tiemin Liu,[1] Mi Hwa Kim,[1] Charlotte E. Lee,[1] Claudia R. Vianna,[1] Kevin W. Williams,[1] Yong Xu,[2,3] and Joel K. Elmquist[1,4]

[1]Division of Hypothalamic Research, Department of Internal Medicine, UT Southwestern Medical Center, Dallas, Texas, USA. [2]Children's Nutrition Research Center, Department of Pediatrics and [3]Department of Molecular and Cellular Biology, Baylor College of Medicine, Houston, Texas, USA. [4]Department of Pharmacology, UT Southwestern Medical Center, Dallas, Texas, USA.

Energy and glucose homeostasis are regulated by central serotonin 2C receptors. These receptors are attractive pharmacological targets for the treatment of obesity; however, the identity of the serotonin 2C receptor–expressing neurons that mediate the effects of serotonin and serotonin 2C receptor agonists on energy and glucose homeostasis are unknown. Here, we show that mice lacking serotonin 2C receptors (*Htr2c*) specifically in pro-opiomelanocortin (POMC) neurons had normal body weight but developed glucoregulatory defects including hyperinsulinemia, hyperglucagonemia, hyperglycemia, and insulin resistance. Moreover, these mice did not show anorectic responses to serotonergic agents that suppress appetite and developed hyperphagia and obesity when they were fed a high-fat/high-sugar diet. A requirement of serotonin 2C receptors in POMC neurons for the maintenance of normal energy and glucose homeostasis was further demonstrated when *Htr2c* loss was induced in POMC neurons in adult mice using a tamoxifen-inducible POMC-*cre* system. These data demonstrate that serotonin 2C receptor–expressing POMC neurons are required to control energy and glucose homeostasis and implicate POMC neurons as the target for the effect of serotonin 2C receptor agonists on weight-loss induction and improved glycemic control.

Introduction

Pharmacological compounds that target central serotonin (5-hydroxytryptamine [5-HT]) signaling potently regulate energy homeostasis and have been used effectively as antiobesity drugs in humans (1). A prime example is d-fenfluramine (d-Fen), which acts to broadly amplify central serotonin bioavailability and was widely used in combination with phenteramine (Fen-Phen) to successfully induce weight loss. Unfortunately, d-Fen and other nonspecific serotonergic agonists were linked to adverse cardiovascular side effects and were withdrawn from clinical use (2, 3). Subsequent work has focused on dissecting how serotonin and d-Fen modulate a complex central serotonergic system, composed of 14 different serotonin receptor isoforms in multiple cell types, to stimulate weight loss (4, 5). These efforts have pinpointed the fact that serotonin and d-Fen act predominantly via central serotonin 2C receptors (6–8) and downstream melanocortin pathways to suppress feeding, thus reducing body weight (9–11). The serotonin 2C receptor agonist Belviq (lorcaserin) is the first FDA-approved drug to treat obesity in 15 years and is a highlight of the persistent interest in central serotonin 2C receptors (12).

In addition to effects on body weight, central serotonin 2C receptors also regulate glucose homeostasis and thus may represent a rational target for type 2 diabetes (T2D) treatment (13, 14). For example, administration of d-Fen and the more specific serotonin 2C receptor agonist m-chloro-phenylpiperazine (mCPP) improves insulin sensitivity and glucose homeostasis, effects that are independent of changes in body weight (15, 16). These data are complemented by findings that antagonists or genetic loss of serotonin 2C receptors impairs glucose homeostasis (17, 18).

Despite these data, a fundamental issue to be clarified is the identity of first-order serotonin 2C receptor–expressing neuron(s) that are required to regulate energy balance and mediate the anorexic and potentially glucose-lowering effects of this class of compounds. This is an unsettled issue because serotonin 2C receptors are widely expressed in the brain (19). Numerous lines of evidence suggest that serotonin 2C receptors in pro-opiomelanocortin (POMC) neurons constitute a key node governing energy balance and glucose homeostasis. First, POMC neurons in the arcuate nucleus of the hypothalamus (ARH) express serotonin 2C receptors and receive input from other serotonin-immunoreactive nerve terminals (9, 20). Serotonin 2C receptor agonists also stimulate POMC expression in the ARH (16, 21). Recent work in vivo also found that serotonin 2C receptor reactivation specifically in POMC neurons of otherwise serotonin 2C receptor–null mice improves energy and glucose homeostasis and is sufficient to mediate the anorexic effects of d-Fen (11, 22, 23). In the current studies, we directly assessed the requirement for intact serotonin 2C receptor expression in POMC neurons to control energy and glucose homeostasis and to mediate pharmacologically induced hypophagia. To this end, we engineered new mouse models to selectively delete serotonin 2C receptors in POMC neurons during early development or adulthood.

Results

Generation and validation of the Htr2c$^{flox/+}$ mouse. To develop a mouse model that allows Cre recombinase–mediated (*cre*-mediated) specific deletion of serotonin 2C receptors, we inserted two *lox*P

Authorship note: Eric D. Berglund and Chen Liu are co–first authors and Yong Xu and Joel K. Elmquist are co–senior authors.

Conflict of interest: The authors have declared that no conflict of interest exists.

Citation for this article: *J Clin Invest.* 2013;123(12):5061–5070. doi:10.1172/JCI70338.

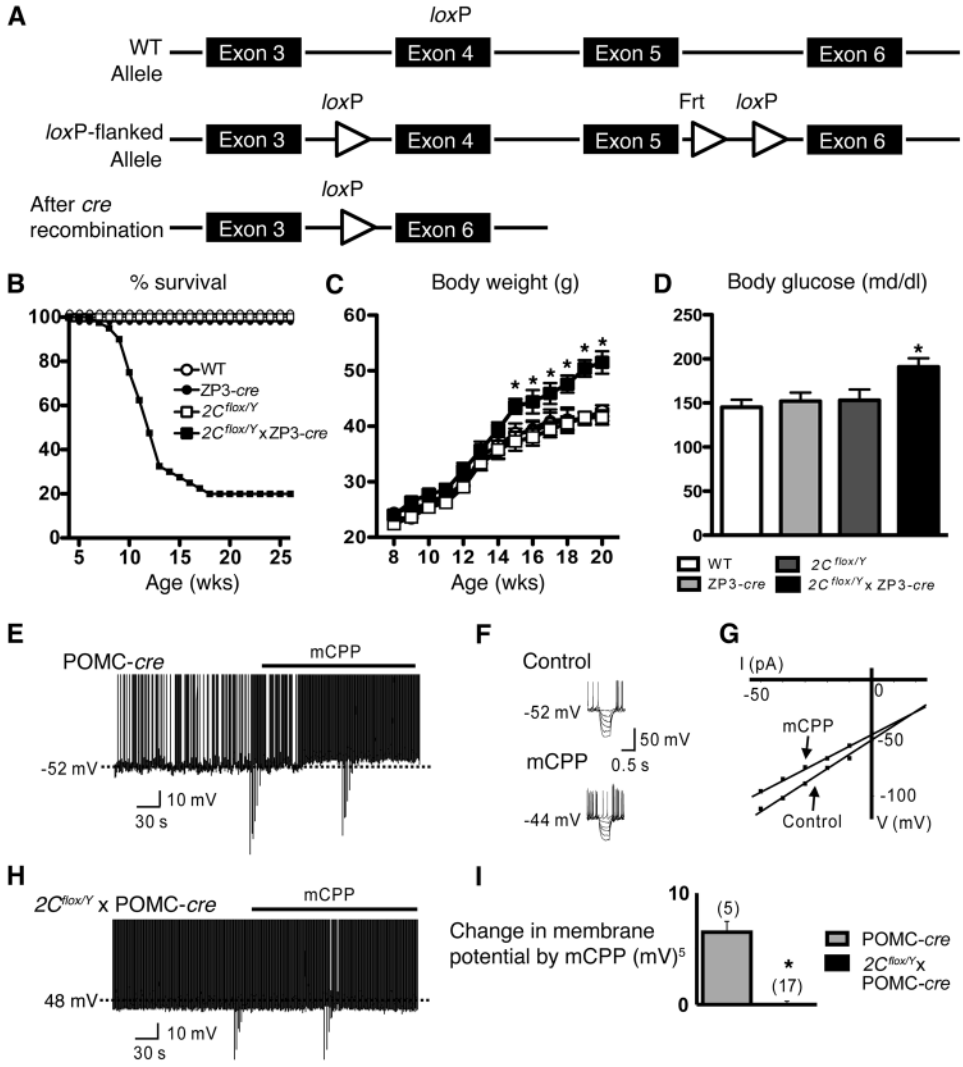

Figure 1
Generation and validation of $2C^{flox/Y}$ mice. (**A**) Strategy used to create mice in which serotonin 2C receptors (*Htr2c* [*2C*]) could be conditionally ablated using *cre-lox* technology. $2C^{flox/Y}$ mice were validated by crossing with mice expressing *cre* in zona pellicuda (ZP3-*cre*) cells to produce whole-body *Htr2c*-null mice ($2C^{flox/Y}$ × ZP3-*cre*). (**B**–**D**) Predicted decreases in survival as well as increases in body weight and 4- to 5-hour-fasted blood glucose levels in $2C^{flox/Y}$ × ZP3-*cre* mice versus littermate controls (n = 17–20 mice/genotype). Symbols in **B** are reduced in size to prevent overlap in the control groups. (**E**–**I**) Six- to 8-week-old male mice lacking *Htr2c* in POMC neurons that coexpress the fluorescent reporter tdTomato were functionally validated using treatment with the serotonin 2C receptor agonist mCPP (4 μM) during electrophysiological recordings. n = 5 POMC-*cre* (controls) and n = 17 $2C^{flox/Y}$ × POMC-*cre* ($2C^{flox}$ × POMC-*cre*) littermate mice in **E**–**I**. Results are shown as the mean ± SEM. *P < 0.05 versus other genotypes assessed using a Student's t test.

sequences to flank exons 4 and 5 of the *Htr2c* gene (Figure 1A). Since *Htr2c* is an X-linked gene, male mice that are hemizygous ($2C^{flox/Y}$) for the floxed *Htr2c* allele are predicted to lack serotonin 2C receptors in all *cre*-expressing cells (24). To validate this mouse model, we first bred male $2C^{+/+}$ mice with female $2C^{flox/+}$ animals expressing *cre* in zona pellucida cells (ZP3-*cre*; ref. 25) to produce whole-body *Htr2c*-null progeny ($2C^{flox/Y}$ × ZP3-*cre*). Progeny were born at Mendelian ratios, and chow-fed $2C^{flox/Y}$ × ZP3-*cre* mice on a mixed C57BL/6J and 129X1/SVJ background exhibited higher mortality rates consistent with seizure-induced death reported in other whole-body serotonin 2C receptor–null mouse models (ref. 6 and Figure 1B). This phenotype was nearly absent in $2C^{flox/Y}$ × ZP3-*cre* mice when backcrossed onto a more enriched C57BL/6J background. Our analyses of $2C^{flox/Y}$ × ZP3-*cre* mice fed an obesigenic high-fat/high-sugar (HFHS) diet also revealed augmented obesity and hyperglycemia versus controls as predicted based on the literature (refs. 7, 23, and Figure 1, C and D).

Next, we bred $2C^{flox/+}$ mice with previously characterized animals in which *cre* is constitutively (developmentally) expressed in POMC neurons (26) to ablate serotonin 2C receptors in this distinct neuronal subset ($2C^{flox}$ × POMC-*cre*). Progeny were born at Mendelian ratios, and there was no evidence of increased mortality in $2C^{flox}$ × POMC-*cre* mice. To validate POMC-specific serotonin 2C receptor deletion, the *cre*-inducible reporter tdTomato allele was bred into male $2C^{flox}$ × POMC-*cre* mice and POMC-*cre* mice, respectively. We then used electrophysiological techniques (22) to record identified POMC neurons in the ARH. We observed the expected cellular responses to mCPP in intact mice (POMC-*cre* × tdTomato), but deletion of serotonin 2C receptors completely blocked these responses in $2C^{flox}$ × POMC-*cre* × tdTomato littermates (Figure 1, E–I, and Supplemental Figure 1, A–C; supplemental material available online with this article; doi:10.1172/JCI70338DS1). Taken together, these data indicate that deletion of serotonin 2C receptors in POMC neurons blocked the ability of mCPP to depolarize POMC neurons and therefore validate the successful development of a mouse model with POMC-specific deletion of serotonin 2C receptors.

Constitutive loss of serotonin 2C receptors in POMC neurons produces hyperphagia and alters energy balance. We first assessed whether deleting serotonin 2C receptors in POMC neurons affects body weight in mice fed a standard chow diet. Body weights in chow-fed $2C^{flox}$ × POMC-*cre* mice were similar to those of the control littermates

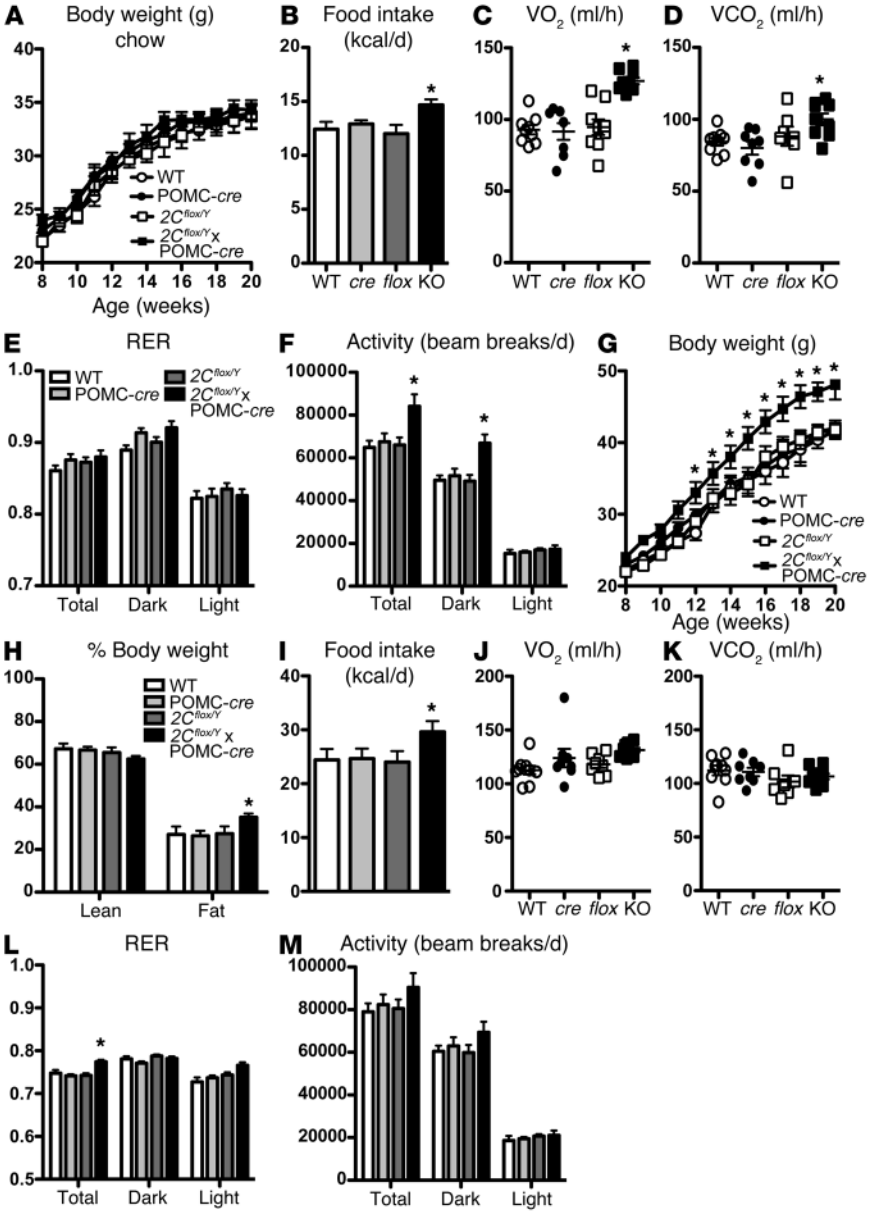

Figure 2
Mice lacking *Htr2c* in POMC neurons exhibit altered energy balance and sensitivity to diet-induced obesity. (**A**–**F**) Body weight and metabolic cage data for 8-week-old male mice lacking *Htr2c* in POMC neurons ($2C^{flox}$ × POMC-*cre*) in chow-fed conditions (n = 8–11 mice per genotype). (**G**–**H**) Body weight and body composition (Bruker minispec) of 20-week-old mice fed an HFHS diet for 8 weeks. (**I**–**M**) Metabolic cage data for 8-week-old mice after 1 week of an HFHS diet (n = 8–11 mice per genotype). Results are shown as the mean ± SEM. *P < 0.05 versus other genotypes assessed using a Student's t test or ANOVA.

upon weaning (4 week of age; data not shown) and were also comparable in these mice between 8 and 20 weeks of age (Figure 2A). We then placed mice of similar body weight (Supplemental Figure 2A) in metabolic cages while fed a chow diet to assess their energy balance. Surprisingly, food intake as well as VO_2, VCO_2, and physical activity were all elevated in the chow-fed $2C^{flox}$ × POMC-*cre* mice (Figure 2, C, D, and F). We found that the respiratory exchange ratio (RER) was similar between the chow-fed groups (Figure 2E). These simultaneous increases in both energy intake and energy expenditure in chow-fed $2C^{flox}$ × POMC-*cre* mice suggest that offsetting mechanisms underlie comparable body weights in chow-fed mice.

We next assessed the responses of the mice following exposure to an HFHS diet. In contrast to the chow-fed mice, the body weight of HFHS-fed $2C^{flox}$ × POMC-*cre* mice increased significantly at approximately 4 weeks after the introduction of the HFHS diet, indicating an increased susceptibility to diet-induced obesity (Figure 2G). HFHS-fed $2C^{flox}$ × POMC-*cre* mice were approximately 25% heavier than controls at 20 weeks of age (12 weeks on an HFHS diet; Figure 2G) due to elevated adiposity (Figure 2H). We next used metabolic cages to determine the mechanisms underlying the increased sensitivity to diet-induced obesity in $2C^{flox}$ × POMC-*cre* mice. We performed experiments first in the chow-fed mice acutely transitioned to an HFHS diet. This strategy resulted in similarly increased body weight after 1 week of an HFHS diet (Supplemental Figure 2B). Acute exposure to an HFHS diet exacerbated only hyperphagia in $2C^{flox}$ × POMC-*cre* mice (Figure 2I). VO_2, VCO_2, and physical activity levels were not elevated compared with the chow condition in the mutant mice (Figure 2, J, K, and M). This lack of response was in contrast to increments of approximately 18% to 20% when comparing VO_2 and physical activity in the chow- and HFHS-fed control genotypes (WT, POMC-*cre*, and $2C^{flox/Y}$ littermates; Figure 2, C, F, J, and M). We found that the

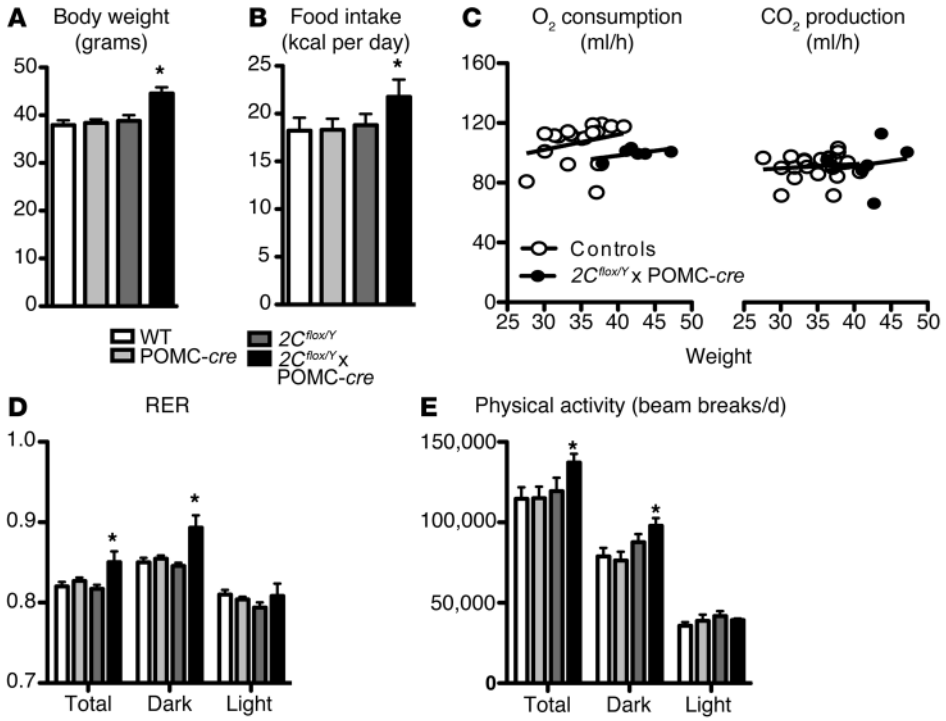

Figure 3
Mice lacking *Htr2c* in POMC neurons and chronically fed an HFHS diet exhibit obesity and altered energy balance. (**A**–**E**) Body weight, food intake, VO_2, VCO_2, and physical activity over a 1-week period in metabolic cages of 20-week-old male mice fed an HFHS diet for 12 weeks (n = 6–9 mice per genotype). Control genotypes (WT, POMC-*cre*, and $2C^{flox/Y}$ littermates) are combined to improve clarity in **C** (no differences exist between these groups). Results are shown as the mean ± SEM. *$P < 0.05$ assessed using Student's t-tests or ANOVA.

RER was reduced in all groups by an HFHS diet, but was modestly higher over a 24-hour period in $2C^{flox}$ × POMC-*cre* mice (Figure 2L). HFHS-induced changes in food intake and VO_2, VCO_2, or physical activity were predominantly due to changes during the dark phase. Taken together, these data suggest that hyperphagia is the primary defect leading to diet-induced obesity in $2C^{flox}$ × POMC-*cre* mice.

To confirm that these acute responses to an HFHS diet are relevant to long-term changes that underlie exaggerated HFHS-induced obesity in $2C^{flox}$ × POMC-*cre* mice, we also performed metabolic cage studies in 20-week-old mice that had been chronically exposed to an HFHS diet for 12 weeks. As expected, body weight in older HFHS-fed $2C^{flox}$ × POMC-*cre* mice was elevated (Figure 3A). In agreement with data obtained in younger, acutely HFHS-fed mice, we found that food intake was elevated in the chronically HFHS-fed 20-week-old $2C^{flox}$ × POMC-*cre* mice (Figure 3B). These changes were due to differences in the dark phase. Analyses of VO_2 relative to body weight in $2C^{flox}$ × POMC-*cre* mice fed an HFHS diet for 12 weeks also revealed lowered rates versus the control cohorts (Figure 3C). VCO_2 rates were similar to those of other genotypes, and these changes in VO_2 and VCO_2 corresponded to a higher RER during the dark phase in HFHS-fed $2C^{flox}$ × POMC-*cre* mice (Figure 3D). Physical activity was also elevated in $2C^{flox}$ × POMC-*cre* mice fed an HFHS diet for 12 weeks exclusively during the dark phase (Figure 3E).

Taken together, these data suggest that chow-fed $2C^{flox}$ × POMC-*cre* mice are hyperphagic, yet maintain a normal body weight due to compensatory adaptations in energy expenditure. We found that hyperphagia was the primary energy balance defect in $2C^{flox}$ × POMC-*cre* mice following HFHS diet exposure, since the HFHS diet augmented hyperphagia, while VO_2, VCO_2, and physical activity were unchanged. These latter results suggest that energetic mechanisms that protect against weight gain in chow-fed mice were already elevated in the $2C^{flox}$ × POMC-*cre* mice. We conclude that these two inputs (increased hyperphagia and maximally strained energy expenditure) combine to produce greater obesity in HFHS-fed $2C^{flox}$ × POMC-*cre* mice.

An additional energy balance–oriented goal of these studies was to better define where d-Fen and more specific serotonin 2C receptor agonists such as mCPP act to suppress food intake. To test the hypothesis that serotonin 2C receptor expression in POMC neurons is required for these effects, we administered d-Fen and mCPP to fasted mice and subsequently examined food intake using a previously described paradigm (23). As expected, d-Fen and mCPP potently suppressed food intake in littermate controls with intact serotonin 2C receptor/POMC signaling (Figure 4). In contrast, this effect was absent in $2C^{flox}$ × POMC-*cre* mice (Figure 4). These findings indicate that d-Fen and mCPP require the serotonin 2C receptors expressed by POMC neurons to acutely suppress food intake.

Selective deletion of serotonin 2C receptors in POMC neurons impairs glucose homeostasis. In addition to controlling energy balance and body weight, prior studies have also suggested that central serotonin 2C receptor signaling directly regulates glucose homeostasis (15–18, 22). Preliminary analyses of blood glucose in ad libitum chow-fed cohorts examined at the beginning of the light cycle (0700 h) showed modestly higher glucose levels in $2C^{flox}$ × POMC-*cre* mice versus littermate controls (Figure 5A). We next examined blood glucose and the glucoregulatory hormones insulin and glucagon in chow-fed mice (where differences in body weight do not exist) as well as in HFHS-fed mice. Blood glucose in chow-fed $2C^{flox}$ × POMC-*cre* mice was modestly, but significantly, elevated in postabsorptive (4- to 5-hour morning-fasted) mice, but was not in 12- or 24-hour overnight-fasted mice (Figure 5A). HFHS feeding provoked a similar rise in blood glucose in postabsorptive (4- to 5-hour morning-fasted) conditions, but this increment versus chow-fed cohorts was comparable, suggesting similar secondary insults (Figure 5A). Similar to blood glucose levels, plasma insulin and glucagon were elevated in postabsorptive mice, but were comparable in

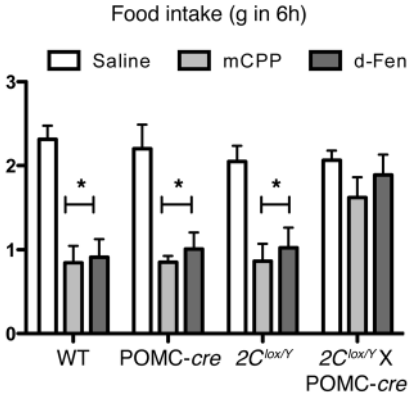

Figure 4
d-Fen and mCPP do not diminish food intake in mice lacking serotonin 2C receptors (*Htr2c*) in POMC neurons. Agonists of serotonin 2C receptor signaling (i.p. d-Fen and mCPP, 5 and 3 mg/kg, respectively) were administered in a counterbalanced manner at 1-week intervals to 18-hour overnight-fasted mice constitutively lacking *Htr2c* specifically in POMC neurons and to control littermates (n = 9–12 mice per genotype). Food was removed at 1800 h, and drug or vehicle was administered at 1130 h the following day. A chow diet was reintroduced 30 minutes later, and food intake was recorded hourly for 6 hours. Data are shown as the means ± SEM. *$P < 0.05$ versus vehicle treatment within a genotype using Student's t tests.

overnight fasted chow-fed $2C^{flox}$ × POMC-*cre* mice (Figure 5, B and C). An HFHS diet also elicited the predicted rise in plasma insulin in postabsorptive conditions, which was exaggerated in $2C^{flox}$ × POMC-*cre* mice (Figure 5B). This latter difference is likely due to greater HFHS-induced obesity in $2C^{flox}$ × POMC-*cre* mice (Figure 2, B and C). An HFHS diet did not, however, further worsen circulating glucagon levels (Figure 5C). We found that plasma leptin levels were comparable in all chow-fed groups, and increases in HFHS diet groups were in accord with differences in adiposity.

We next performed hyperinsulinemic-euglycemic clamps to assess whether insulin sensitivity was impaired in 8- to 9-week-old $2C^{flox}$ × POMC-*cre* mice compared with their $2C^{flox}$ littermates. Previous studies have shown that insulin-mediated suppression of endogenous glucose production and stimulation of glucose disposal are identical in POMC-*cre* mice and their WT littermates (27). These data demonstrate that expression of the POMC-*cre* transgene does not independently affect clamp data. Experiments were performed first in postabsorptive (4- to 5-hour morning-fasted) animals with matched body weights ($2C^{flox}$: 25.0 ± 1.2 g vs. $2C^{flox}$ × POMC-*cre*: 25.1 ± 1.7 g, $P > 0.05$). During the clamp, the incremental rise in insulin levels was comparable between genotypes (Figure 5D). This acute rise in insulin did not, however, suppress hyperglucagonemia in $2C^{flox}$ × POMC-*cre* mice (Figure 5E). Blood glucose was successfully clamped at target levels (Supplemental Figure 3A), and the exogenous glucose infusion rate (GIR) was lower in $2C^{flox}$ × POMC-*cre* mice, indicating a reduced insulin sensitivity (Figure 5F). This difference in GIR was due to impaired insulin-mediated suppression of endogenous glucose appearance (endo R_a) (Figure 5G) and not glucose disappearance (R_d) (Figure 5H). We then conducted a second group of complementary experiments in 8- to 9-week-old 12-hour overnight-fasted mice with matched body weights ($2C^{flox}$: 24.1 ± 0.9 g vs. $2C^{flox}$ × POMC-*cre*: 23.9 ± 1.2 g; $P > 0.05$) to mitigate the potential impact of unsuppressed glucagon levels on the clamped GIR in postabsorptive mice. This strategy was based on earlier findings (Figure 5, B and C) that basal plasma insulin and glucagon levels would be comparable in this context. As shown in Figure 5, I and J, this strategy was successful in normalizing both clamp steady-state plasma insulin and glucagon levels. We again performed hyperinsulinemic-euglycemic clamps at target levels (Supplemental Figure 3B), and the required GIR was reduced in $2C^{flox}$ × POMC-*cre* mice (Figure 5K). The magnitude of the reduced clamp steady-state GIR compared between genotypes in 12-hour-fasted mice (32%) was modestly higher than in the 5-hour-fasted cohorts (26%). This higher GIR, indicating insulin resistance in 12-hour-fasted $2C^{flox}$ × POMC-*cre* mice, was due to both impaired insulin-mediated suppression of the endogenous rate of glucose endo R_a and a 16% reduction in the endogenous rate of glucose R_d (Figure 5, L and M). Together, these clamp experiments, in which glucagon levels did not always differ, indicate a modest contribution to impaired postprandial insulin suppression of endo R_a.

Collectively, these findings demonstrate that intact serotonin 2C receptor expression in POMC neurons is required to maintain normal glucose regulation. The fact that the mice studied were of comparable body weights demonstrates that the effects of serotonin 2C receptors on glycemic control are independent of their effects on body weight. These data highlight the notion that hyperglycemia is associated with both relative hyperglucagonemia and hyperinsulinemia as well as with a consistent impairment in insulin-stimulated endogenous glucose production. It is noteworthy that an HFHS diet further exacerbates hyperinsulinemia and therefore likely further impairs dysregulated insulin-mediated control of glucose flux, as indicated by hyperinsulinemic-euglycemic clamp studies in chow-fed mice.

Inducible loss of serotonin 2C receptors in POMC neurons in adult mice recapitulates aberrant energy and glucose homeostasis. We next asked whether adult-onset loss of serotonin 2C receptors in POMC neurons results in a phenotype similar to that of ablation during development. This is a key issue, because recent work has found that multiple lineages of hypothalamic neurons express POMC, including cells that may not express POMC in adult mice (28). Additionally, recent studies have shown that pre- and postnatal ablation of AgRP neurons results in disparate feeding behavior phenotypes (29). These latter findings suggest that phenotypes caused by prenatal ablation may be influenced by developmental compensation in central pathways that regulate food intake (29). To circumvent some of these issues, we developed a tamoxifen-inducible POMC-*cre* mouse model (POMC-*cre:ER*^{T2}) that allows temporal control of *cre* recombinase activity and can be combined with $2C^{flox}$ mice to enable adult-onset deletion. To validate this model, we administered tamoxifen to POMC-*cre:ER*^{T2} mice that coexpress the reporter tdTomato to provoke *cre* expression and assessed them using immunohistochemical techniques. We detected no *cre* activity in the vehicle-treated controls (data not shown). In contrast, tamoxifen treatment of POMC-*cre:ER*^{T2} mice induced expression of the *cre*-dependent reporter tdTomato (Figure 6A). We detected *cre* activity in greater than 95% of POMC neurons in the ARH (Figure 6, B and C), indicating successful development of the mouse model.

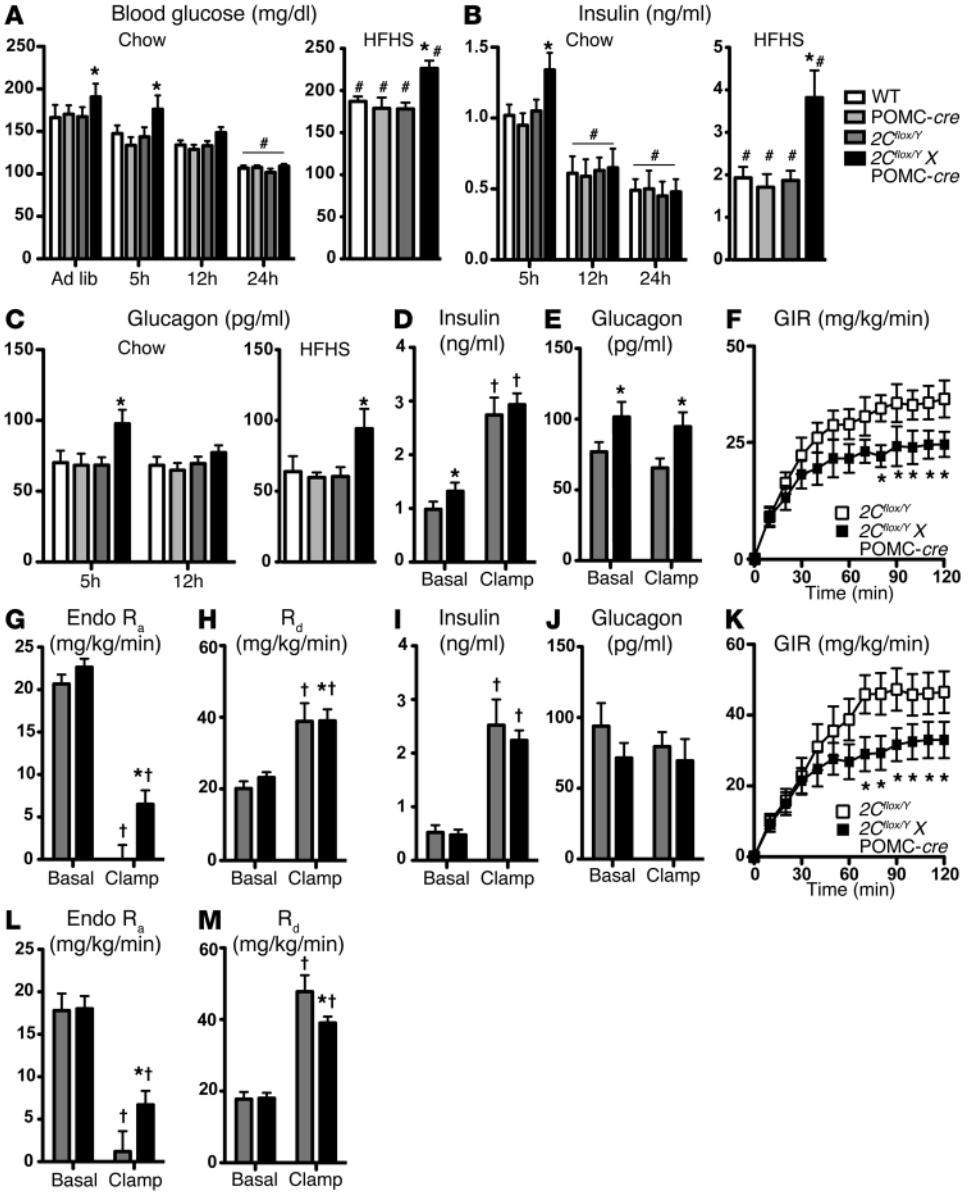

Figure 5
Impaired glucoregulation in mice lacking serotonin 2C receptors (*Htr2c*) specifically in POMC neurons. (**A**–**C**) Blood glucose, plasma insulin, and plasma glucagon in chow- and HFHS-fed conditions respectively; n = 9–12 mice per genotype per diet. Ad libitum (Ad lib) blood glucose values in **A** represent measurements taken at 0700 h. Postabsorptive values represent a 4- to 5-hour morning fast, and 12- and 24-hour fasts denote removal of food at 2100 h or 1800 h, respectively, the night before in **A**–**C**. HFHS values in **A**–**C** are from 4- to 5-hour-fasted mice. (**D** and **E**) Basal and clamp plasma insulin and glucagon levels in 4- to 5-hour morning-fasted (0800–0900 h to 1300 h; n = 7–8 mice per genotype), chronically catheterized, conscious mice during a 120-minute hyperinsulinemic-euglycemic (4 mU/kg/minute, 150 mg/dl, respectively) clamp. (**F**) Exogenous GIR needed to clamp blood glucose. (**G** and **H**) Endogenous rates of endo R_a and R_d were determined using a constant infusion of [3-^{3}H]glucose and steady-state calculations. (**I**–**M**) Similar clamp parameters for 12-hour overnight-fasted (2100 h–0900 h; n = 7–8 mice per genotype). Blood was taken from the cut tail, and results are shown as the mean ± SEM. $^*P < 0.05$ versus other genotypes, $^\#P < 0.05$ versus ad libitum and/or 5-hour-fasted chow-fed conditions within a genotype, and $^\dagger P < 0.05$ versus basal values during hyperinsulinemic-euglycemic clamp using Student's t tests.

This novel mouse model was then used to induce adult-onset loss of serotonin 2C receptors in POMC neurons ($2C^{flox}$ × POMC-*cre:ER*^{T2}). In agreement with data using constitutive POMC-*cre* mice, the administration of tamoxifen to 11-week-old mice to induce adult-onset loss serotonin 2C receptors in POMC neurons did not affect body weight in the 12- to 20-week-old chow-fed cohorts (Figure 6D). We then placed these mice in metabolic cages to study energy balance in cohorts with similar body weights (Supplemental Figure 4A). In agreement with the data in chow-fed constitutive POMC-*cre* cohorts (see Figure 2), we found that the chow-fed $2C^{flox}$ × POMC-*cre:ER*^{T2} mice exhibited higher food intake, VO_2, and VCO_2 (Figure 6, E–G). These elevations were due to differences in the dark phase. Neither the RER nor physical activity was different (Supplemental Figure 4, B and C).

We next assessed another cohort of $2C^{flox}$ × POMC-*cre:ER*^{T2} mice treated with tamoxifen at 11 weeks of age and switched to an HFHS diet 1 week after the first dose. In agreement with the data in the HFHS-fed constitutive POMC-*cre* cohorts (see Figure 2), HFHS-fed $2C^{flox}$ × POMC-*cre:ER*^{T2} mice exhibited increased body weight after 6 weeks of HFHS feeding (Figure 6H). Additionally, our metabolic cage studies in acutely HFHS-fed mice recapitulated our earlier findings in $2C^{flox}$ × POMC-*cre* mice (see Figure 2). Specifically, an HFHS diet stimulated hyperphagia, but did not further increase VO_2 and VCO_2 in $2C^{flox}$ × POMC-*cre:ER*^{T2} mice (Figure 6, I–K), whereas HFHS feeding in control mice led to approximately 11% to 13% rises in VO_2 and VCO_2 (Figure 6, F, G, J, and K). In addition, consistent with observations from mice with constitutive deletion of serotonin 2C receptors in POMC neurons, chow-fed $2C^{flox}$ × POMC-*cre:ER*^{T2} mice displayed similar deficits in glycemic control. Thus, both blood glucose and glucagon levels were elevated 2 weeks after tamoxifen injections (mice were 13 weeks of age; Figure 7, A and B), while hyperinsulinemia was evident after 4 weeks (Figure 7C).

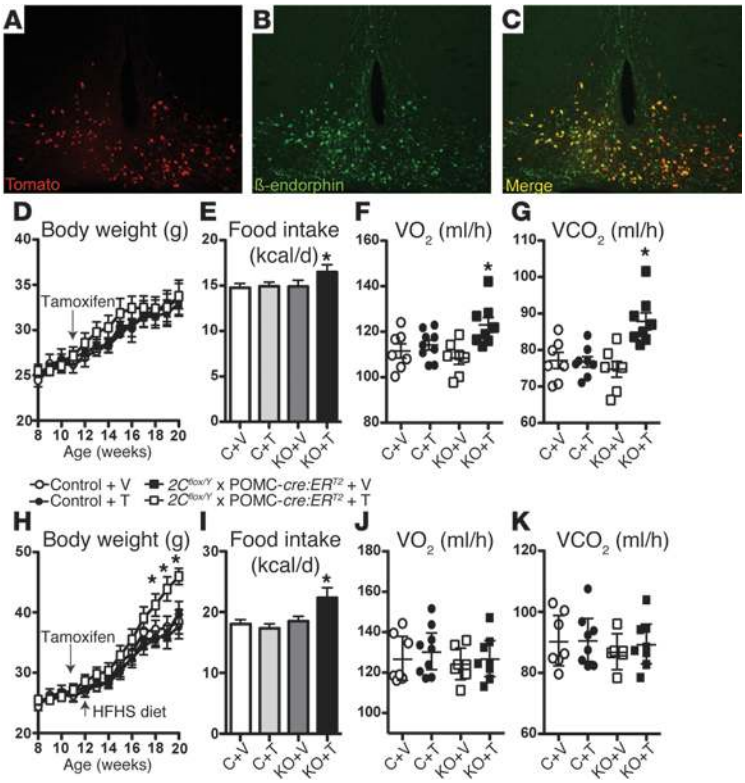

Figure 6
Inducible deletion of serotonin 2C receptors (*Htr2c*) in POMC neurons of adult mice dysregulates energy homeostasis. Tamoxifen-inducible POMC-*cre* (POMC-*cre*:ER^{T2}) mice that coexpress the *cre*-stimulated fluorescent reporter tdTomato were treated with 0.15 mg/kg tamoxifen (T) i.p. daily for 5 days, and immunohistochemistry was used to assess the expression of Tomato (**A** and **C**) and β-endorphin (**B** and **C**). Male POMC-*cre*:ER^{T2} (**C**) and $2C^{flox/Y}$ x POMC-*cre*:ER^{T2} (KO) littermate mice were then treated with tamoxifen or vehicle (V) at 11 weeks of age to assess their chow-fed body weight (**D**). This was repeated to assess metabolic cages studies in chow-fed mice (**E**–**G**; n = 7–9 mice per genotype). Male POMC-*cre*:ER^{T2} (WT) and $2C^{flox/Y}$ x POMC-*cre*:ER^{T2} ($2C^{flox/Y}$) littermate mice were also fed an HFHS diet to assess body weight (**H**). (**I**–**K**) Metabolic cage data following 1-week exposure to an HFHS diet (n = 7–9 per genotype). Results are shown as the means ± SEM. *$P < 0.05$ versus other genotypes using Student's t tests.

Taken together, these findings demonstrate that the metabolic outcomes induced by pre- and postnatal deletion of serotonin 2C receptors in POMC neurons are strikingly comparable. These data strengthen the evidence showing that loss of serotonin 2C receptors in POMC neurons induces modest hyperphagia that is insufficient to surpass the homeostatic control mechanisms regulating body weight. Obesigenic challenges such as an HFHS diet, however, exacerbate hyperphagia and overwhelm the protective processes that maintain normal body weight. These data also suggest that serotonin 2C receptor signaling in POMC neurons controls blood glucose as well as glucagon and insulin levels. Our data show that increased glucagon was the first observable change in the circulation.

Discussion

The current studies demonstrate that serotonin 2C receptor signaling in POMC neurons is required to maintain normal energy and glucose homeostasis. Selective loss of serotonin 2C receptor signaling in POMC neurons provokes hyperphagia, sensitizes mice to diet-induced obesity, and directly (i.e., independently of changes in body weight) dysregulates glucose homeostasis with elevations in circulating glucagon, insulin, and blood glucose. In addition to these physiological aberrations, loss of serotonin 2C receptor expression in POMC blunts the effects of d-Fen and mCPP to suppress food intake. Notably, these results were obtained using novel mouse models ($2C^{flox/+}$ and POMC-*cre*:ER^{T2} mice). Since serotonin 2C receptors are expressed widely in the CNS, $2C^{flox/+}$ mice should prove to be a useful tool for studying the role of serotonin 2C receptors in other regions of the nervous system. In addition, the POMC-*cre*:ER^{T2} mouse model circumvents issues regarding differential phenotypes comparing constitutive versus adult-onset deletion (29). The use of this mouse facilitates the ability to possibly temporally assess the effects of genetic manipulations of a number of genes in POMC neurons at different developmental and adult ages.

It is interesting that mice with global serotonin 2C receptor deficiency developed late-onset obesity when fed a chow diet (>26 weeks of age) and that this phenotype was accelerated by an obesigenic diet (6, 23). Since the serotonin 2C receptors expressed in POMC neurons are one of many targets of endogenous serotonin, it was not surprising that chow-fed $2C^{flox}$ × POMC-*cre* and $2C^{flox}$ × POMC-*cre*:ER^{T2} mice maintained normal body weight. It was surprising, however, that body weights in the $2C^{flox}$ × POMC-*cre* and $2C^{flox}$ × POMC-*cre*:ER^{T2} mice fed an obesigenic diet diverged from those of their littermate controls earlier than in the global serotonin 2C receptor–null mice ($2C^{flox}$ × ZP3-*cre* mice; Figure 1B) and also diverged earlier than previously reported timelines in other global serotonin 2C receptor–null models (6, 23).

It is also noteworthy that our examination of the chow- and HFHS-fed $2C^{flox}$ × POMC-*cre* and $2C^{flox}$ × POMC-*cre*:ER^{T2} mice supports and extends prior conclusions that serotonin 2C receptor neural circuits predominantly control feeding. Both $2C^{flox}$ × POMC-*cre* and $2C^{flox}$ × POMC-*cre*:ER^{T2} mice exhibited hyperphagia in chow-fed contexts that was exacerbated by an obesigenic challenge. Relative increases in VO_2 and VCO_2 were also evident in chow-fed $2C^{flox}$ × POMC-*cre* and $2C^{flox}$ × POMC-*cre*:ER^{T2} mice, but these processes were unaltered by an HFHS diet. These findings suggest that homeostatic control of feeding is deranged, while hedonic processes sensitive to an HFHS diet remain intact in mice lacking serotonin 2C receptors in POMC neurons. A related conclusion is that energy expenditure in both $2C^{flox}$ × POMC-*cre* and $2C^{flox}$ × POMC-*cre*:ER^{T2} mice remains functional to counteract the heightened energy intake seen in chow-fed contexts, but cannot further

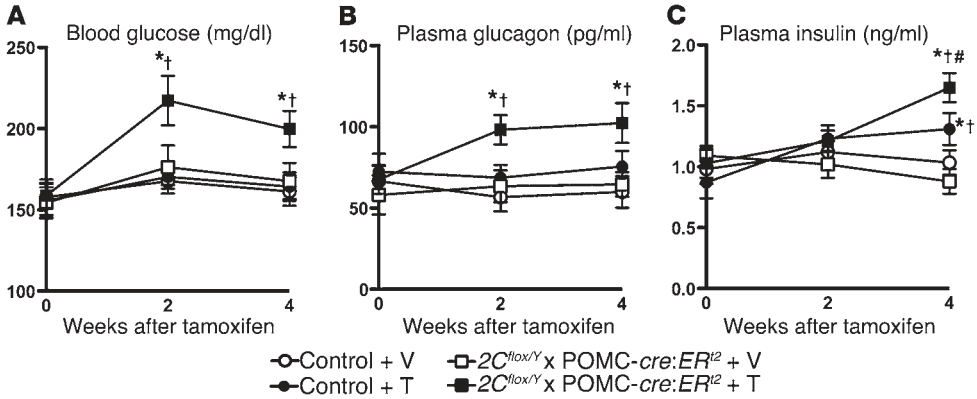

Figure 7
Inducible deletion of serotonin 2C receptors (*Htr2c*) in POMC neurons of adult mice dysregulates glucose homeostasis. Tamoxifen-inducible POMC-*cre* (POMC-*cre*:ER^{T2}) mice and their respective controls (n = 8 mice per genotype) were treated with tamoxifen (0.15 mg/kg i.p. daily for 5 days) or vehicle. Blood samples from the cut tail were taken immediately before the first dose (week 0) as well as 2 and 4 weeks after treatment to measure plasma glucagon and insulin levels. Results are shown as the means ± SEM. *P < 0.05 versus other genotypes and P < 0.05 versus other genotypes; †P < 0.05 versus pre-tamoxifen treatment values within the genotype; #P < 0.05 versus tamoxifen-treated control mice.

increase to account for the additional energy intake in HFHS circumstances. These data, in concert with other studies focusing on POMC neuron–mediated regulation of feeding, suggest a complex neuronal circuitry in the ARH. The current data support models in which POMC neurons in the ARH control feeding. This is in contrast to recent data demonstrating that leptin receptor signaling via POMC neurons does not control food intake, but only energy expenditure (27, 30). Of note is the finding that serotonin 2C receptors and leptin receptors are expressed by anatomically and functionally distinct POMC neurons in the ARH (31, 32), but they converge on similar second-order neurons, including those expressing melanocortin 4 receptors (MC4Rs). It is currently unclear how serotonin 2C receptor– and leptin receptor–positive POMC neurons differentially control overlapping downstream pathways and/or interlinked physiological processes. Loss of leptin receptor signaling in POMC neurons modestly affects body weight (26, 30). Genetic loss of leptin receptors alone in POMC neurons does not produce a major glucoregulatory phenotype (26, 30). However, loss of both insulin and leptin receptors in POMC neurons does induce hepatic insulin resistance (30). In contrast, serotonin 2C receptor signaling in POMC neurons requires an obesigenic challenge for a body-weight phenotype, but these mice do exhibit glucoregulatory defects in chow-fed conditions.

We also found that both d-Fen and mCPP, drugs with serotonin 2C receptor agonist properties, were ineffective at suppressing feeding in $2C^{flox}$ × POMC-*cre* mice. This was somewhat surprising because d-Fen and mCPP treatments were anticipated to provoke an intermediate hypophagic response in $2C^{flox}$ × POMC-*cre* mice, given the multiple other serotonin 2C receptor–expressing sites of action. These results suggest that d-Fen and mCPP critically require serotonin 2C receptor expression in POMC neurons to suppress feeding. These data are topical because the highly specific serotonin 2C receptor agonist lorcaserin was approved recently as an antiobesity therapeutic agent by the FDA and is now available for prescription use in humans. Other pending antiobesity drugs that include combination therapies of bupropion and naltrexone or zonisamide also function to stimulate POMC neurons via different mechanisms and thus provoke weight loss (33). We anticipate that these current results as well as our new experimental tools described here will be relevant to future efforts at discerning the specifics about site(s) and mechanism(s) of action of these and potentially other drugs that target central serotonin 2C receptors.

Another salient finding in both the $2C^{flox}$ × POMC-*cre* and $2C^{flox}$ × POMC-*cre*:ER^{T2} models is the evidence supporting primary defects in glucose regulation. It is of note that differences in blood glucose were restricted to postabsorptive conditions in $2C^{flox}$ × POMC-*cre* mice (not in overnight-fasted conditions), a pattern consistent with feeding-induced increases in central serotonin release and bioavailability (34). Analyses of factors that contribute to glycemic control revealed that mice lacking serotonin 2C receptors in POMC neurons were hyperinsulinemic, hyperglucagonemic, and insulin resistant. Glucagon was measured because of its effects on glucose metabolism (35), recent evidence that leptin (27) and glucagon-like peptide 2 (GLP-2) (36) act via POMC neurons to alter plasma glucagon, and because of renewed interest in the pathogenic contributions of the hormone to diabetes (37). Our temporal analyses of these parameters following tamoxifen treatment in $2C^{flox}$× POMC-*cre*:ER^{T2} mice suggest that an early rise in blood glucagon levels may at least partly contribute to hyperglycemia. These data are noteworthy because prior work has established that central MC4R signaling, the putative downstream pathway engaged by serotonin 2C receptor–positive POMC neurons, directly regulates the endocrine pancreas (38, 39). The clamp results are noteworthy, however, because they indicate that hepatic insulin resistance is the primary glucoregulatory defect in $2C^{flox}$ × POMC-*cre* mice and suggest that glucagon contributes to, but does fully account for, this phenotype. Interestingly, the current estimation that the maximum glucagon-stimulated contribution to elevated clamp endo R_a in postabsorptive $2C^{flox}$ × POMC-*cre* mice is approximately 20% is on par with recent work assessing the role(s) of relative hyperglucagonemia in clamp data (27, 36). The relevance of these data in mice is bolstered by work showing that failed suppression of glucagon contributes to postprandial hyperglycemia in humans with T2D (40, 41).

Overall, these data demonstrate that aberrant glucose homeostasis exists independently of altered body weight in mice lacking serotonin 2C receptors in POMC neurons and suggest that aberrant postprandial blood glucose is multifactorial and includes hyperglucagonemia — albeit in a modest manner — and impaired insulin-mediated hepatic glucose suppression. These findings support and extend a growing body of literature showing that direct glucose regulatory effects are linked to central serotonin 2C receptors and POMC neurons. Future work is needed to dissect which neural/hormonal mechanism(s) underlie these changes and which tissue(s)/cell type(s) are primary site(s) of dysregulation. Numerous possible mechanisms include sympathetic and parasympathetic inputs to the liver, pancreas, and/or other organs. One admittedly simplified model to explain these findings is that loss of serotonin 2C receptors in POMC neurons prevents feeding-induced activation of MC4Rs in the sympathetic and parasympathetic preganglionic neurons, resulting in unsuppressed liver glucose production as well as insulin and glucagon secretion.

In summary, our conclusions that serotonin 2C receptors are required in POMC neurons to maintain normal energy and glucose homeostasis complement and extend prior work showing that the reactivation of serotonin 2C receptors in POMC neurons in mice that otherwise lack serotonin 2C receptors is sufficient to correct energy and glucose homeostatic defects. Collectively, our results provide definitive in vivo evidence and an expanded framework for understanding how physiologically or pharmacologically induced changes in the regulation of serotonin 2C receptors in POMC neurons impact energy balance and glycemic control. These data are important in understanding the biological basis for the increasing prevalence of obesity and T2D and the current therapeutic strategies used to target these diseases.

Methods

Animal care. The IACUC committee of the UT Southwestern Medical Center (UTSW) approved all animal procedures. The mice were bred and housed in a barrier facility on a 12-hour light/12-hour dark cycle and were provided standard chow (2016; Harlan Teklad) or an HFHS (D12331; Research Diets) as well as water ad libitum unless otherwise noted.

Generation of a cre-conditional Htr2c-null allele. The lox-modified *Htr2c*-targeting plasmid was constructed using a BAC clone containing genomic *Htr2c* sequences derived from the 129X1/SvJ mouse strain. All cloning steps were performed using homologous recombination in SW106 bacteria. The start codon of the *Htr2c* is in exon 4, thus two *lox*P sites were inserted into introns 3 and 5, respectively. Lox-modified *Htr2c* DNA was cloned using pGEM-T easy vector (Promega) and transfected into ES cells at the UTSW Transgenic Core Facility.

Generation of an inducible POMC-cre model. Tamoxifen-inducible *cre:ER^{T2}* (42) mice controlled by *Pomc* regulatory elements (26) were developed to temporally control *cre* excision specifically in POMC-expressing neurons. Founder lines with inducible *cre* activity were screened by injecting 6-week-old *cre* reporter mice from these lines (*R26R$^{tdTomato+}$* [tdTomato] × POMC-*cre:ER^{T2}*) with a single daily dose of tamoxifen (0.15 mg/kg body weight) or vehicle (corn oil) for 5 consecutive days. The expression of tdTomato 15 days after the final dose of tamoxifen was detected in nearly all POMC neurons (>95%) in the ARH as well as in a small number of neurons in the brainstem. Recombination was strictly dependent upon tamoxifen treatment, as no *cre* activity could be detected in the absence of tamoxifen. *cre* activity was also not detected in other regions of the CNS after tamoxifen injections. *cre*-activated reporter expression was present in the pituitary gland where the *Pomc* gene was endogenously expressed.

Tamoxifen treatment to induce adult-onset ablation of Htr2c in POMC neurons. Tamoxifen (0.15 mg/kg; Sigma-Aldrich) suspended in corn oil (Sigma-Aldrich) was administered i.p. for 5 consecutive days to 11-week-old male *2C^{flox}* mice (controls) and *2C^{flox}* × POMC-*cre:ER^{T2}* littermate mice. Corn oil was used as a vehicle control.

Body composition. Body composition was assessed using NMR (minispec; Bruker).

Survival analysis. Survival was assessed from the age of weaning until the final week of observation (4–26 weeks).

Electrophysiology. Electrophysiological recordings were made as previously described (31).

Metabolic cage experiments. Energy expenditure and food intake were measured using a 36-chamber metabolic chamber system (TSE Systems) at the UTSW Mouse Phenotyping Core facility. Mice were individually housed for 1 week prior to a 3-day acclimation period in TSE cages. Mice were then assessed for 5 days while fed a chow diet. Body weight was measured on day 5 in chow-fed conditions and an HFHS diet was introduced and monitoring continued for an additional 7 days.

Blood glucose and hormone analyses. Blood glucose and plasma hormones were analyzed from blood either collected from the cut tail or via cardiac puncture when the experiment was terminal. Blood glucose was analyzed using an AlphaTRAK meter (Abbott Laboratories) designed for use with rodents. Plasma insulin and leptin levels were measured using an ELISA kit designed for use in mice (Crystal Chem, Inc.) at the UTSW Mouse Phenotyping Core facility. Plasma glucagon was measured using a double-antibody RIA at the Vanderbilt University Mouse Metabolic Phenotyping Center Hormone Assay and Analytical Core facility.

Hyperinsulinemic-euglycemic clamps. Hyperinsulinemic-euglycemic clamps were performed at the UTSW Mouse Phenotyping Core in conscious, chronically catheterized mice using previously described techniques (30). Postabsorptive experiments were conducted in mice in which food was removed between 0800 h and 0900 h to begin a 4- to 5-hour fast. Overnight-fasted experiments were conducted in mice in which food was removed at 2100 h (2.5 hours after lights off) to begin a 12-hour fast. [3-^{3}H]glucose (PerkinElmer) was infused beginning at t = –120 minutes to calculate basal and insulin-stimulated glucose turnover. Humulin R (4 mU/kg/minute; Eli Lilly) was used to induce hyperinsulinemia. Dextrose (50%) was infused to maintain target blood glucose levels. Blood samples were taken from the cut tail.

Analyses of d-Fen– and mCPP-induced hypophagia. d-Fen (5 mg/kg; Sigma-Aldrich), mCPP (3 mg/kg; Sigma-Aldrich), and vehicle (sterile saline) were administered i.p. in a counterbalanced manner to chow-fed 18-hour overnight-fasted mice as previously described (11). Food was introduced 30 minute after treatment to individually housed mice, and food intake was measured hourly for 6 hours.

Statistics. Survival data are depicted in a Kaplan-Meier curve and were assessed using a log-rank test. Days 2–4 of chow-fed conditions and days 3–5 of HFHS-fed conditions were used to assess differences, if any, between genotypes and/or dietary conditions in metabolic cage experiments. Basal and insulin-stimulated endo R_a and R_d during hyperinsulinemic-euglycemic clamps were calculated using Steele's steady-state equation (43). All results were analyzed using Student's t tests or ANOVA where appropriate. All data are presented as the mean ± SEM, where $P < 0.05$ was considered statistically significant.

Acknowledgments

The authors would like to thank the staff of the UTSW Mouse Phenotyping Core. We also thank the NIH for its support (DK 059637) of the Vanderbilt University Mouse Metabolic Pheno-

typing Core and Hormone Assay and Analytical Services Core facilities. This work was also supported by NIH grant NIDDK F32 DK092083 (to E.D. Berglund); a postdoctoral fellowship from the Hilda and Preston Davis Foundation (to C. Liu); a mentor-based postdoctoral fellowship grant from the American Diabetes Association (7-11-MN-16, to T. Liu); NIH grants NIDDK R01 DK093587 and R00 DK085330; an American Diabetes Association grant (1-11-BS-180); and a Klarman Family Foundation grant (to Y. Xu); as well as by NIH grants NIDDK R01 DK088423 and R37 DK053301 (to J.K. Elmquist).

Received for publication July 25, 2013, and accepted August 22, 2013.

Address correspondence to: Joel K. Elmquist, UT Southwestern/Room Y6.322, 5323 Harry Hines Blvd., Dallas, Texas 75390-9077, USA. Phone: 214.648.2911; Fax: 214.648.5612; E-mail: joel.elmquist@utsouthwestern.edu. Or to: Yong Xu, Children's Nutrition Research Center, Department of Pediatrics, Baylor College of Medicine, 1100 Bates Street, Rm 8070, Houston, Texas 77030, USA. Phone: 713.798.7199; Fax: 713.798.7187; E-mail: yongx@bcm.edu.

1. Halford JC, Boyland EJ, Lawton CL, Blundell JE, Harrold JA. Serotonergic anti-obesity agents: past experience and future prospects. *Drugs*. 2011; 71(17):2247–2255.
2. Connolly HM, et al. Valvular heart disease associated with fenfluramine-phentermine. *N Engl J Med*. 1997; 337(9):581–588.
3. James WP, et al. Effect of sibutramine on cardiovascular outcomes in overweight and obese subjects. *N Engl J Med*. 2010;363(10):905–917.
4. Bello NT, Liang NC. The use of serotonergic drugs to treat obesity — is there any hope? *Drug Des Devel Ther*. 2011;5:95–109.
5. Garfield AS, Heisler LK. Pharmacological targeting of the serotonergic system for the treatment of obesity. *J Physiol*. 2009;587(pt 1):49–60.
6. Tecott LH, et al. Eating disorder and epilepsy in mice lacking 5-HT2c serotonin receptors. *Nature*. 1995; 374(6522):542–546.
7. Nonogaki K, Strack AM, Dallman MF, Tecott LH. Leptin-independent hyperphagia and type 2 diabetes in mice with a mutated serotonin 5-HT2C receptor gene. *Nat Med*. 1998;4(10):1152–1156.
8. Vickers SP, Clifton PG, Dourish CT, Tecott LH. Reduced satiating effect of d-fenfluramine in serotonin 5-HT(2C) receptor mutant mice. *Psychopharmacology (Berl)*. 1999;143(3):309–314.
9. Heisler LK, et al. Activation of central melanocortin pathways by fenfluramine. *Science*. 2002; 297(5581):609–611.
10. Heisler LK, et al. Serotonin reciprocally regulates melanocortin neurons to modulate food intake. *Neuron*. 2006;51(2):239–249.
11. Xu Y, et al. A serotonin and melanocortin circuit mediates D-fenfluramine anorexia. *J Neurosci*. 2010; 30(44):14630–14634.
12. Colman E, Golden J, Roberts M, Egan A, Weaver J, Rosebraugh C. The FDA's assessment of two drugs for chronic weight management. *N Engl J Med*. 2012; 367(17):1577–1579.
13. Marston OJ, Garfield AS, Heisler LK. Role of central serotonin and melanocortin systems in the control of energy balance. *Eur J Pharmacol*. 2011; 660(1):70–79.
14. Lam DD, Heisler LK. Serotonin and energy balance: molecular mechanisms and implications for type 2 diabetes. *Expert Rev Mol Med*. 2007;9(5):1–24.
15. Storlien LH, Thorburn AW, Smythe GA, Jenkins AB, Chisholm DJ, Kraegen EW. Effect of d-fenfluramine on basal glucose turnover and fat-feeding-induced insulin resistance in rats. *Diabetes*. 1989; 38(4):499–503.
16. Zhou L, et al. Serotonin 2C receptor agonists improve type 2 diabetes via melanocortin-4 receptor signaling pathways. *Cell Metab*. 2007;6(5):398–405.
17. Wade JM, et al. Synergistic impairment of glucose homeostasis in ob/ob mice lacking functional serotonin 2C receptors. *Endocrinology*. 2008; 149(3):955–961.
18. Wozniak KM, Linnoila M. Hyperglycemic properties of serotonin receptor antagonists. *Life Sci*. 1991; 49(2):101–109.
19. Molineaux SM, Jessell TM, Axel R, Julius D. 5-HT1c receptor is a prominent serotonin receptor subtype in the central nervous system. *Proc Natl Acad Sci U S A*. 1989;86(17):6793–6797.
20. Kiss J, Léránth C, Halász B. Serotoninergic endings on VIP-neurons in the suprachiasmatic nucleus and on ACTH-neurons in the arcuate nucleus of the rat hypothalamus. A combination of high resolution autoradiography and electron microscopic immunocytochemistry. *Neurosci Lett*. 1984; 44(2):119–124.
21. Lam DD, et al. Serotonin 5-HT2C receptor agonist promotes hypophagia via downstream activation of melanocortin 4 receptors. *Endocrinology*. 2008; 149(3):1323–1328.
22. Xu Y, et al. 5-HT2CRs expressed by pro-opiomelanocortin neurons regulate insulin sensitivity in liver. *Nat Neurosci*. 2010;13(12):1457–1459.
23. Xu Y, et al. 5-HT2CRs expressed by pro-opiomelanocortin neurons regulate energy homeostasis. *Neuron*. 2008;60(4):582–589.
24. Kawahara Y, et al. Dysregulated editing of serotonin 2C receptor mRNAs results in energy dissipation and loss of fat mass. *J Neurosci*. 2008; 28(48):12834–12844.
25. de Vries WN, et al. Expression of Cre recombinase in mouse oocytes: a means to study maternal effect genes. *Genesis*. 2000;26(2):110–112.
26. Balthasar N, et al. Leptin receptor signaling in POMC neurons is required for normal body weight homeostasis. *Neuron*. 2004;42(6):983–991.
27. Berglund ED, et al. Direct leptin action on POMC neurons regulates glucose homeostasis and hepatic insulin sensitivity in mice. *J Clin Invest*. 2012; 122(3):1000–1009.
28. Padilla SL, Carmody JS, Zeltser LM. Pomc-expressing progenitors give rise to antagonistic neuronal populations in hypothalamic feeding circuits. *Nat Med*. 2010;16(4):403–405.
29. Luquet S, Perez FA, Hnasko TS, Palmiter RD. NPY/AgRP neurons are essential for feeding in adult mice but can be ablated in neonates. *Science*. 2005; 310(5748):683–685.
30. Hill JW, et al. Direct insulin and leptin action on pro-opiomelanocortin neurons is required for normal glucose homeostasis and fertility. *Cell Metab*. 2010;11(4):286–297.
31. Sohn JW, Xu Y, Jones JE, Wickman K, Williams KW, Elmquist JK. Serotonin 2C receptor activates a distinct population of arcuate pro-opiomelanocortin neurons via TRPC channels. *Neuron*. 2011; 71(3):488–497.
32. Williams KW, et al. Segregation of acute leptin and insulin effects in distinct populations of arcuate proopiomelanocortin neurons. *J Neurosci*. 2010; 30(7):2472–2479.
33. Heal DJ, Gosden J, Smith SL. What is the prognosis for new centrally-acting anti-obesity drugs? *Neuropharmacology*. 2012;63(1):132–146.
34. Schwartz DH, Hernandez L, Hoebel BG. Serotonin release in lateral and medial hypothalamus during feeding and its anticipation. *Brain Res Bull*. 1990; 25(6):797–802.
35. Jiang G, Zhang BB. Glucagon and regulation of glucose metabolism. *Am J Physiol Endocrinol Metab*. 2003; 284(4):E671–E678.
36. Shi X, et al. Central GLP-2 enhances hepatic insulin sensitivity via activating PI3K signaling in POMC neurons. *Cell Metab*. 2013;18(1):86–98.
37. Unger RH, Cherrington AD. Glucagonocentric restructuring of diabetes: a pathophysiologic and therapeutic makeover. *J Clin Invest*. 2012;122(1):4–12.
38. do Carmo JM, da Silva AA, Rushing JS, Hall JE. Activation of the central melanocortin system contributes to the increased arterial pressure in obese Zucker rats. *Am J Physiol Regul Integr Comp Physiol*. 2012;302(5):R561–R567.
39. Fan W, Dinulescu DM, Butler AA, Zhou J, Marks DL, Cone RD. The central melanocortin system can directly regulate serum insulin levels. *Endocrinology*. 2000;141(9):3072–3079.
40. Shah P, Basu A, Basu R, Rizza R. Impact of lack of suppression of glucagon on glucose tolerance in humans. *Am J Physiol*. 1999;277(2 pt 1):E283–E290.
41. Shah P, Vella A, Basu A, Basu R, Schwenk WF, Rizza RA. Lack of suppression of glucagon contributes to postprandial hyperglycemia in subjects with type 2 diabetes mellitus. *J Clin Endocrinol Metab*. 2000; 85(11):4053–4059.
42. Feil R, Brocard J, Mascrez B, LeMeur M, Metzger D, Chambon P. Ligand-activated site-specific recombination in mice. *Proc Natl Acad Sci U S A*. 1996; 93(20):10887–10890.
43. Steele R, Wall JS, De Bodo RC, Altszuler N. Measurement of size and turnover rate of body glucose pool by the isotope dilution method. *Am J Physiol*. 1956; 187(1):15–24.